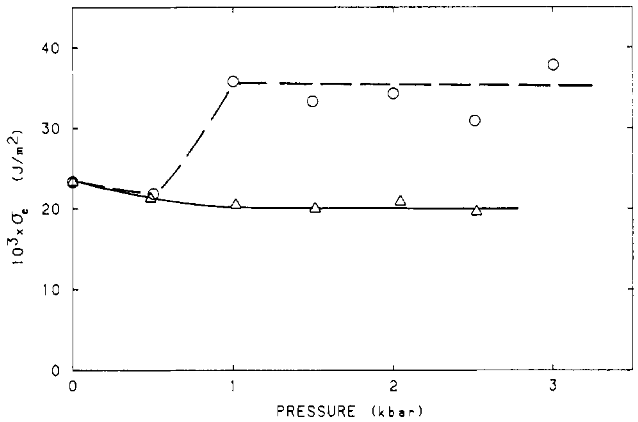

Figure 12. Pressure dependence of the fold surface free energy σ_e: (△) thermodynamic data (P_c = 1 bar); (○) lamellar thickness data ($P_c = P_m$).

pressure thereafter. This behavior is remarkable but is quite distinctly evident.

While σ_e data can, in principle, also be determined from T_m vs. $1/l$ data for material crystallized at high pressure, this analysis is seriously limited by practical considerations. The high-pressure lamellar thickness data available[11] is at relatively large undercoolings, in general well outside the short range of temperatures at which approximately linear T_m vs. T_c data are obtained. This eliminates a direct correlation between the melting and lamellar thickness data, and an extrapolation procedure is required. Several further approximations are needed to calculate σ_e values at high pressure, which are found to lie near 0.027 J/m^2, which is about midway between the two limiting values (0.020 and 0.035) in Figure 12. In view of the gross approximations involved, this inconclusive result is not unexpected; the increase in σ_e is nevertheless qualitatively evident.

A model involving a pressure-induced change in the crystal fold conformation has been proposed[3] to explain the behavior of σ_e at high pressure. This model will be discussed in a later publication; however, it is possible at this time to state that the observed jump is easy to reconcile with an adjacent reentry fold but does not seem to be compatible with a switchboard mode.

References and Notes

(1) C. K. L. Davies and M. C. M. Cucarella, *J. Mater. Sci.*, **15**, 1547 (1980).
(2) E. N. Dalal, K. D. Taylor, and P. J. Phillips, *Polymer*, in press.
(3) E. N. Dalal, Ph.D. Dissertation, University of Utah, 1983.
(4) W. B. Daniels, private communication.
(5) G. J. Granieri, RCA Electronic Components Manual ICAN-4158, 1969.
(6) H.-G. Kim and L. Mandelkern, *J. Polym. Sci., Part A-2*, **10**, 1125 (1972).
(7) B. Wunderlich, "Macromolecular Physics", Academic Press, New York, 1980, Vol. 3.
(8) H. Tadokoro, "Structure of Crystalline Polymers", Wiley-Interscience, New York, 1979.
(9) J. D. Hoffman, G. T. Davis, and J. I. Lauritzan, Jr., in "Treatise on Solid State Chemistry", N. B. Hannay, Ed., Plenum Press, New York, 1976, Vol. 3, Chapter 7.
(10) F. E. Karasz and L. D. Jones, *J. Phys. Chem.*, 71, 2234 (1967).
(11) P. J. Phillips and B. C. Edwards, *J. Polym. Sci., Polym. Phys. Ed.*, **13**, 1819 (1975).

Efficient Use of Two-Dimensional Detectors for Small-Angle Neutron Scattering Contours from Polymers under External Constraint

D. F. R. Mildner

Research Reactor Facility and Department of Physics, University of Missouri, Columbia, Missouri 65211. *Received March 7, 1983*

ABSTRACT: Small-angle neutron scattering is a technique for studying polymer chain conformation using mixtures of protonated and deuterated species. When the polymer is under some external constraint, different radii of gyration are determined along directions of the scattering vector parallel and perpendicular to the stretching axis. Published experiments use only data along these two directions, and most of the data collected on two-dimensional detectors are thrown away. For a system with an axis of rotational symmetry (polymers under uniaxial stretch), the scattering cross section has elliptical symmetry at small scattering vectors. An analysis with the radius of gyration having elliptical azimuthal dependence makes efficient use of two-dimensional detectors. An elliptical fitting technique is useful particularly when part of the important data is not accessible on the spectrometer.

Amorphous polymer chains are described by random Gaussian conformation, and it is of current interest to know how this conformation changes under external constraint.[1-8] The plastic deformation behavior of polymers can be studied in two ways, isotropic deformation (e.g., swelling) or anisotropic deformation (e.g., uniaxial stretching or compression). Small-angle neutron scattering (SANS) has become a popular technique for studying the polymer chain conformation in the solid state using mixtures of protonated and deuterated species to determine the radius of gyration. The spherical averaging inherent in isotropic systems causes details in the molecular conformation to remain undetected. In highly oriented systems the conformation of the individual polymer chain depends on its orientation relative to the constraint. It is found that different radii of gyration are determined along directions of the scattering vector parallel and perpendicular to the axis of stretching or compression. The molecular theory of polymer elasticity states that the deformation is affine; that is, the dimensions of the molecular chains deform in direct proportion to the macroscopic dimensions of the sample.

SANS measurements frequently use large-area position-sensitive detectors. The intensity of scattered radiation is recorded as a two-dimensional contour (that is, as a function of scattering and azimuthal angles) representing

0024-9297/83/2216-1760$01.50/0

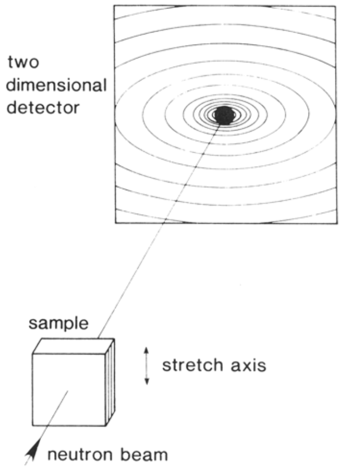

Figure 1. Schematic diagram of a small-angle neutron scattering experiment on a uniaxially stretched polymer sample, showing the elliptical contours on the two-dimensional detector.

distances characteristic of the inhomogeneities in the plane normal to the direction of the incident beam. This is illustrated in Figure 1. When the sample is anisotropic, as in stretched or oriented polymers, it is customary to analyze the scattering in different azimuthal directions.[9] The two-dimensional detector is divided up into small azimuthal sectors $\Delta\phi$, and only those sectors parallel and perpendicular to the stretch axis are used, so that not all the data are used. Much longer counting times are required for equal statistical accuracy than for experiments on isotropic samples where the counts per cell are larger because the intensity is averaged over all the detector cells.

These longer counting times are unnecessary, since it can be shown that all the data can be used to determine the necessary parameters. For preferentially oriented inhomogeneities, the scattered intensity will have elliptical azimuthal symmetry, with major and minor axes corresponding to distances in the scattering plane characteristic of the inhomogeneities.[10] The observation of ellipitically symmetric scattering contours implies only that there is some preferred direction of the inhomogeneities about which there is, an average, rotational symmetry. We summarize the theory given elsewhere[11] and apply the results to recent publications.[5-7]

The scattered intensity measured at the detector is proportional to the Fourier transform of the scattering density function of the system. The general expression for the scattering cross section $S(\mathbf{Q})$ may be expanded for small values of the scattering vector $\mathbf{Q}$. Reflection symmetry and the introduction of the pair correlation function $g(\mathbf{r})$ for the inhomogeneities allow the scattering cross section to be written in terms of an integral $\int \mathrm{d}^3\mathbf{r}\, g(\mathbf{r})\cdot(\mathbf{Q}\cdot\mathbf{r})^2$. If it assumed that $g(\mathbf{r})$ is independent of azimuth, that is, on the average the inhomogeneities have rotational symmetry about an axis (the stretching or compression axia, then $g(\mathbf{r})$ depends only on the scalar distance r and the polar angle, but not on the azimuthal angle. Integration over the azimuthal angle gives an expression for the scattering cross section that is dependent only on the polar angle θ_0 of the scattering vector $\mathbf{Q}$ relative to the sample symmetry axis

$$\begin{aligned} S(\mathbf{Q}) &= [1 + (a^2 \cos^2 \theta_0 + b^2 \sin^2 \theta_0)Q^2]^{-1} \\ &= [1 + R_G{}^2(\theta_0)Q^2]^{-1} \qquad (1) \end{aligned}$$

The constants a and b are independent of the polar angle θ_0 of the vector $\mathbf{Q}$ and are related to the second moments of the pair correlation function. Note that if the pair correlation function is assumed to be independent of the polar angle (that is, the scattering system is isotropic so that $g(\mathbf{r})$ depends only on scalar r), the two constants are identical, and the cross section is given by

$$S(\mathbf{Q}) = [1 + a^2Q^2]^{-1} \qquad (2)$$

the familiar Guinier approximation at low Q.

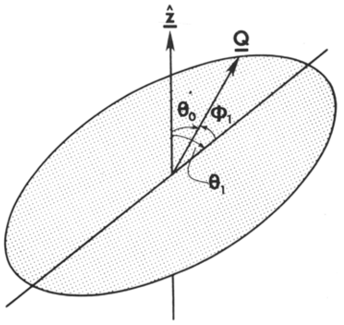

Figure 2. Schematic diagram showing (i) the scattering plane at an angle θ_1 to the sample axis $\hat{\mathbf{z}}$ and (ii) the scattering vector $\mathbf{Q}$ with a polar angle θ_0 relative to the symmetry axis and an azimuthal angle ϕ_1 within the scattering plane, such that $\cos\theta_0 = \cos\theta_1 \cos\phi_1$.

We can define R_Q, the radius of gyration of the inhomogeneities in the plane of the scattering vector $\mathbf{Q}$, by

$$R_Q{}^2 \int \mathrm{d}^3\mathbf{r}\, g(\mathbf{r}) = \int \frac{(\mathbf{Q}.\mathbf{r})^2}{Q^2}\, \mathrm{d}^3\mathbf{r}\, g(\mathbf{r}) \qquad (3)$$

The value of the radius of gyration depends on the angle θ_1 of the scattering plane relative to the symmetry axis of the sample (see Figure 2). The polar angle θ_0 of the vector $\mathbf{Q}$ is given by

$$\cos\theta_0 = \cos\theta_1 \cos\phi_1 \qquad (4)$$

where ϕ_1 is the azimuthal angle of $\mathbf{Q}$ within the scattering plane. Integration over the azimuthal angle of the vector $\mathbf{r}$ relative to the symmetry axis gives the result

$$R_G{}^2(\theta_1,\phi_1) = (a^2 \cos^2\theta_1 + b^2 \sin^2\theta_1) \cos^2\phi_1 + b^2 \sin^2\phi_1 \qquad (5)$$

showing that the radius of gyration has azimuthal (ϕ_1) dependence on the scattering vector $\mathbf{Q}$, as well as angular (θ_1) dependence of the scattering plane relative to the sample symmetry axis. This gives rise to scattering contours with elliptical symmetry and with the radius of gyration having an eccentricity given by $(a^2 \cos^2\theta_1 + b^2 \sin^2\theta_1)^{1/2}/b$. Note that when the symmetry axis lies perpendicular to the scattering plane ($\hat{\mathbf{z}} \perp \mathbf{Q}$), then $\theta_1 = \pi/2$, and $R_{Q\perp}{}^2 = R_{G\perp}{}^2 = b^2$. The scattering is symmetric, independent of azimuth, and the two-dimensional data may be averaged radially to give measured radius of gyration $R_{G\perp}$. When the symmetry axis lies in the scattering plane, then $\theta_1 = 0$, $\phi_1 = \theta_0$, and $R_{Q\parallel}{}^2 = R_{G\parallel}{}^2 \cos^2\theta_0 + R_{G\perp}{}^2 \sin^2\theta_0$, where θ_0 is now the azimuth. The scattering has elliptical azimuthal symmetry, and the measured radii of gyration along and perpendicular to the axis of symmetry are $R_{G\parallel}$ and $R_{G\perp}$. Note also that for an isotropic system where $g(r)$ depends only on scalar r that the integration of eq 3 gives

$$R_Q{}^2 = \frac{1}{3} \frac{\int_0^\infty r^4 g(r)\, \mathrm{d}r}{\int_0^\infty r^2 g(r)\, \mathrm{d}r} = \frac{1}{3} R_{G0}{}^2 \qquad (6)$$

In general, there is no reason to suppose that the correlation function of chains within an amorphous polymer placed under some external constraint has lower than rotational symmetry. Hence such data can be analyzed by the foregoing analysis. Given the elliptical form of the Guinier approximation, we have shown that the cross section may be written

$$S(\mathbf{Q})^{-1} = 1 + [R_{G\parallel}{}^2 \cos^2 \theta_1 + R_{G\perp}{}^2 \sin^2 \theta_1) \cos^2 \phi_1 + R_{G\perp}{}^2 \sin^2 \phi_1]Q^2 \quad (7)$$

where $R_{G\parallel}$ and $R_{G\perp}$ are the radii of gyration of the inhomogeneities when the scattering vector $\mathbf{Q}$ is parallel and perpendicular to the sample symmetry axis, θ_1 is the angle the scattering plane makes with the symmetry axis, and ϕ_1 the azimuthal angle of the scattering vector. Generally, measurements are taken for samples with the symmetry axis in the scattering plane to give $R_{G\parallel}$ and $R_{G\perp}$ directly. Only those parts of the data that lie along the two perpendicular directions are used and the rest thrown away. It is better to use the entire two-dimensional data and fit them to a function of the form of eq 7. We now apply this analysis to some recently published results.

SANS measurements to characterize plastic deformation of amorphous polymer require deuterated-labeled species to be added, so that the radii of gyration of the deurated component are determined in directions parallel and perpendicular to the unique axis. The earlier results[1-4] show that around the onset of uniaxial stretch, $S(\mathbf{Q})^{-1}$ is linear in Q^2 and that for small draw ratios (<3) the deformation is purely affine at low temperatures. However, the contribution of nonaffine mechanisms increases with temperature. This suggests two types of plastic deformation behavior of polymers: (1) at lower temperatures polymer chains slip relative to each other (individual chains elongate by unfolding) for which it is possible to define a unique axis, and (2) at higher temperatures there is also diffusion (individual chains move relative to each other) which has no preferred direction defined on the molecular level.

Lefebvre et al.[6] report SANS measurements to characterize plastic deformation of amorphous polystyrene under compression which result in a shear band. They find that the diffusional mode shows no asymmetry with $R_{G\parallel} \sim R_{G\perp} \sim R_{G0}$, whereas the slip mode results in marked asymmetry, given by the eccentricity $R_{G\perp}/R_{G\parallel}$. The elliptical contours of the data should be related to the elements of the strain tensor.

Hadziioannou et al.[5] have performed SANS measurements on coextrusion oriented polystyrene. They find good agreement between the effective draw ratio (EDR) and the molecular draw ratio (MDR) determined from SANS measurements. This is confirmation of the affine model, indicating that under the drawing conditions used, the radii of gyration deform in the same manner as the external dimensions. In terms of the radius of gyration R_{G0} of the undrawn polymer, which is isotropic, the scattered intensity for the extruded polymer when the extrusion direction lies in the scattering plane may be given by

$$S(\mathbf{Q})^{-1} = 1 + \tfrac{1}{3}R_{G0}{}^2Q^2[(\mathrm{MDR})^2 \cos^2 \theta_0 + (\mathrm{MDR})^{-1} \sin^2 \theta_0] \quad (8)$$

where θ_0 is the azimuthal angle relative to the drawing axis. All the accessible data can be fitted by this equation, and the ratio of the major and minor axis of the elliptical contours gives the molecular draw ratio; that is, $R_{G\parallel}/R_{G\perp} = (\mathrm{MDR})^{3/2}$. These equations are valid, of course, whether the polymer deforms affinely or not.

On the other hand, Ballard et al.[7] have reported SANS measurements on the molecular conformation in hot drawn polypropylene samples which exhibit marked asymmetry in the diffraction pattern. However, they find only modest elongation of the molecule (MDR) compared to the extension of the polymer sample (EDR), in contrast to the results of Hadziioannou et al.[5] on polystyrene. This is probably because both modes of deformation have taken place. Though their data were taken on two perpendicular linear position-sensitive detectors, the scattering contours, if measured, would have shown elliptical symmetry.

Hadziioannou et al.[5] report that the falloff of the scattered intensity corresponding to the direction parallel to the extrusion sometimes occurs at too small values of scattering vector to allow a direct measurement of the radius of gyration in the drawing direction for large $R_{G\parallel}$. The scattering at very low Q can be obscured by the beam stop, particularly for samples of large molecular weight with a large effective draw ratio. The use of a two-dimensional detector and an elliptical fit allows all the accessible data to be used to give both the MDR and the values of the radii of gyration in both directions.

Sadler and Barham[8] have given an alternative technique to analyze asymmetric data that are partially obscured by the beam stop, for the customary experimental condition of the symmetry axis laying in the scattering plane. If the draw ratio is very large such that $R_{G\parallel} \gg R_{G\perp}$, then the form of an off-axis cut perpendicular to the major axis (along the draw direction) may be approximated by $1 + R_{G\parallel}{}^2Q^2$. Again, this method only uses a small fraction of the available data and is only valid for highly asymmetric scatterers.

The use of the Guinier equation with azimuthal asymmetry requires the definition of an axis to the scattering contours and a determination of the aspect ratio to define a molecular draw ratio. The use of such a fit allows all the data available on the detector to be used so that the run times for comparable statistics can be brought closer to those of the isotropic polymer samples. While this paper shows the usefulness of the method in the Guinier region ($QR_G < 1$), it is also applicable to the intermediate Q region where the intensities are lower. This technique will also be useful for time-dependent measurements for the study of polymer dynamics.[12]

The above analysis assumes perfect resolution data, and errors in the determination of the radii of gyration may arise when corrections for both angular and wavelength resolution of the spectrometer are ignored. The contribution of the angular resolution is independent of scattering vector, whereas the contribution of the wavelength resolution increases linearly with scattering vector. Provided $\Delta\lambda/\lambda$ is relatively small ($\sim$10%), the error in the measured values of R_G using this analysis without resolution corrections is also small, since the data fall off relatively slowly in scattering vector. On the other hand, if measurements are made with $\Delta\lambda/\lambda \sim 50\%$, the resolution broadening is considerable, resulting in lower measured values of R_G. In addition, there may also be errors caused by multiple scattering, though it has been shown[13] that for typical experimental conditions these are small.

Acknowledgment. The author acknowledges an interaction with G. C. Summerfield. Acknowledgment is made to the donors of the Petroleum Research Fund, administered by the American Chemical Society, for the partial support of this research.

Registry No. Neutron, 12586-31-1.

References and Notes

(1) Benoit, H.; Duplessix, R.; Ober, R.; Daoud, M.; Cotton, J. P.; Farnoux, B.; Jannink, G. *Macromolecules* **1975**, *8*, 451–453.

(2) Picot, C.; Duplessix, R.; Decker, D.; Benoit, H.; Boué, F.; Cotton, J. P.; Daoud, M.; Farnoux, B.; Jannink, G.; Nierlich, M.; de Vries, A. J.; Pincus, P. *Macromolecules* **1977**, *10*, 436–442.

(3) Hinckley, J. A.; Han, C. C.; Mozer, B.; Yu, H. *Macromolecules* **1978**, *11*, 836–838.
(4) Clough, S. B.; Maconnachie, A.; Allen, G. *Macromolecules* **1980**, *13*, 774–775.
(5) Hadziioannou, G.; Wang, L.-H.; Stein, R. S.; Porter, R. S. *Macromolecules* **1982**, *15*, 880–882.
(6) Lefebvre, J. M.; Escaig, B.; Picot, C. *Polymer* **1982**, *23*, 1751–1754.
(7) Ballard, D. G. H.; Cheshire, P.; Janke, E.; Nevin, A.; Schelten, J. *Polymer* **1982**, *23*, 1875–1883.
(8) Sadler, D. M.; Barham, P. J. *J. Polym. Sci., Polym. Phys. Ed.* **1983**, *21*, 309–317.
(9) Maconnachie, A.; Richards, R. W. *Polymer* **1978**, *19*, 739–762.
(10) Hall, P. L.; Mildner, D. F. R. *J. Appl. Phys.* **1983**, *54*, 427–428.
(11) Summerfield, G. C.; Mildner, D. F. R. *J. Appl. Crystallogr.* **1983**, *16*, 384–389.
(12) Boué, F.; Nierlich, M.; Jannink, G.; Ball, R. C. *J. Phys. (Paris), Lett.* **1982**, *43*, L585–L591.
(13) Goyal, P. S.; King, J. S.; Summerfield, G. C. *Polymer* **1983**, *24*, 131–134.

Effect of Loop Entropy on the Helix–Coil Transition of α-Helical, Two-Chain, Coiled Coils. 2. Supermatrix Formulation of the Perfect-Matching Model

Jeffrey Skolnick

Department of Chemistry, Washington University, St. Louis, Missouri 63130.

Received February 17, 1983

ABSTRACT: The loops-excluded model of the α-helix to random coil transition of α-helical, two-chain, coiled coils (dimers) in which loop entropy acts to produce a single interacting helical stretch in the dimer has been reformulated in terms of the supermatrix method of Jernigan and Flory. It is demonstrated that the loops-excluded model is a member of the class of nearest-neighbor models. Serial matrix product expressions for the internal partition function of the dimer, Z_{sd}, the overall helix content, f_{hd}, the helix probability profiles, and the ratio, R_{d}, of the number of residues that are part of randomly coiled runs at the chain ends to the total number of random coils are derived. The supermatrix method is demonstrated to possess none of the numerical instabilities of our previously developed extension of the Poland recursion relation method to two-chain, coiled coils. Application of the supermatrix formalism to homopolymers demonstrates that all the conclusions of the loops-excluded model based on the recursion relation method remain unchanged. In the limit that R_{d} lies near unity, the neglect-loop-entropy theory (in which loop entropy is entirely ignored) and the loops-excluded model are identical. When R_{d} is significantly less than one, loop entropy makes the helix–coil transition more cooperative; thus values of the helix–helix interaction parameter w extracted from experiment and employing the neglect-loop-entropy theory may be significantly in error, overestimating the helix–helix interaction at high helix content and underestimating it at low helix content.

I. Introduction

In a previous work (hereafter designated paper I), using a modification of Poland's recursion relation method,[1] the theory of the α-helix to random coil transition in two-chain, coiled coils was extended to include the effect of loop entropy.[2] The important qualitative conclusion that emerges from the study is that in two-chain, coiled coils (dimers) of short to moderate length, the entropic cost of forming interior random coil loops between interacting helical stretches is so prohibitive as to eliminate them entirely. Thus, there is a single interacting helical stretch in the dimer, perhaps preceded or followed by noninteracting helical stretches punctuated by interior random coil sequences. The model that possesses these features is called the "loops-excluded model". While the qualitative conclusions are correct, certain numerical instabilities inherent in the recursion relation method as modified and applied to two-chain, coiled coils were found. In this paper we present an alternative matrix method that not only eliminates these numerical instabilities but is computationally faster, and we also, and much more importantly, demonstrate that the loops-excluded model is a nearest-neighbor interaction model, thus enabling us to employ matrix techniques developed previously.[2-4] The matrix method will be applied to homopolymeric, two-chain, coiled coils and compared with calculations made via the Poland recursion relation method and with the neglect-loop-entropy theory.

As a detailed discussion and justification of the underlying physical ideas that form the basis of the loops-excluded model has been given previously, we refer the reader to paper I, with particular emphasis on sections I and V. We content ourselves here with a brief review of the salient features of the helix–helix interaction.

The α-helical, two-chain, coiled coil tropomyosin is known to have a quasi-repeating heptet in the primary sequence that has been designated by the letters "a–g".[5-8] Positions "a" and "d" are almost always occupied by hydrophobic residues; position "e" is almost always anionic and position "g" cationic. The interaction of the hydrophobic residues "a" and "d" with their hydrophobic counterparts on the adjacent chain, "a′" and "d′", respectively, and the possible salt bridge formation of residues "e" and "g" with "g′" and "e′", respectively, on the adjacent chain are believed to be responsible for the greatly enhanced helix content of the dimer relative to the isolated single chains, i.e., monomers (the latter calculated from Zimm–Bragg helix–coil transition theory[9] using the σ and s values as determined by Scheraga et al.[10-23]). To incorporate the essential physics of the interaction into the theory, the two-chain, coiled coil is divided into alternating four- (a–d) and three-residue blocks (e–g) and treated by the coarse-graining method originally developed by Crothers and Kallenbach.[24] Thus we require that residues "a–d" (or "e–g") be in the all-helical state on both chains to effect the enhanced stability characterized by a parameter w. Thus, the coarse graining is not, as in the case of DNA, an approximation employed to simplify the calculations; rather it is a statement of the fundamental physics of the interaction.

Two problems are encountered when Poland's recursion relation method is applied to two-chain, coiled coils, and

0024-9297/83/2216-1763$01.50/0